Biogeosciences Discuss., https://doi.org/10.5194/bg-2018-134
Manuscript under review for journal Biogeosciences
Discussion started: 25 April 2018

Impacts of anthropogenic inputs on the hypoxia and oxygen dynamics in the Pearl River Estuary

Bin Wang [1,3], Jiatang Hu [1,2,*], Shiyu Li [1,2,*], Liuqian Yu[3], Jia Huang [1]

[1] School of Environmental Science and Engineering, Sun Yat-Sen University, Guangzhou, 510275, China
[2] Guangdong Provincial Key Laboratory of Environmental Pollution Control and Remediation Technology, Guangzhou 510275, China
[3] Department of Oceanography, Dalhousie University, Halifax, Nova Scotia, Canada

Correspondence to: Jiatang Hu (hujtang@mail.sysu.edu.cn), Shiyu Li (eeslsy@mail.sysu.edu.cn)

Abstract. In summer, the Pearl River Estuary experiences hypoxia, largely driven by the high input of freshwater with low dissolved oxygen (DO) and abundant nutrients and particulate organic carbon from the Pearl River network. In this study, we used a well-validated coupled physical-biogeochemical model to study the response of hypoxia and oxygen dynamics to variations of anthropogenic inputs (i.e. DO, nutrients, and particulate organic carbon). Model results showed that hypoxia in the Pearl River Estuary was confined to the shelf off the Modaomen sub-estuary with a hypoxic area of ~200 km^2 mainly due to the combined effect of re-aeration and sediment oxygen demand. Numerical experiments suggested that hypoxia in the Pearl River Estuary was most sensitive to riverine inputs of particulate organic carbon , followed by DO concentrations and nutrients. Specifically, a 50% decrease (increase) in riverine input of particulate organic carbon led to a 47% decrease (64% increase) in hypoxic area, with the sediment oxygen demand and water column production being the two most important processes contributing to the changes in DO concentration and hypoxic extent. Changes in the riverine inputs of DO and nutrients had little impact on the simulated hypoxia because of the buffering effects of re-aeration, i.e. the re-aeration compensated the changes in surface apparent oxygen utilization (AOU) associated with river-induced variations of oxygen source and sink processes. The Pearl River Estuary features shallow waters (with averaged depth of 10 m) where oxygen provided by the re-aeration could penetrate to bottom waters via vertical diffusion that largely offset the changes in DO contributed by other oxygen source and sink processes. This study highlights the importance of re-aeration in determining the hypoxic extent and the buffering effects of re-aeration in reducing hypoxia variability in shallow estuary.

Biogeosciences Discuss., https://doi.org/10.5194/bg-2018-134
Manuscript under review for journal Biogeosciences
Discussion started: 25 April 2018

Copyright statement. We certify that this paper consists of original, unpublished work which is not under consideration for publication elsewhere. All authors have seen the final version of the manuscript and approved to submit to your journal.

1. Introduction

Recent decades have seen a decline in dissolved oxygen (DO) concentrations in most of the coastal oceans, leading to an increase in the occurrence and intensity of hypoxic conditions (Diaz and Rosenberg, 2008). The decline in DO concentrations in coastal oceans may be caused by the large-scale climate variations, or driven by the excessive nutrient input associated with human activities (Diaz and Rosenberg, 2008; Rabalais et al., 2010). For instance, climate variations can change the ocean circulation or the upwelling intensity to alter the balance between the oxygen supply and consumption (Rabalais et al., 2010), and change water column stratification that has strong impact on hypoxia development (Du and Shen, 2015). As to human activities, the excessive nutrient input to coastal oceans facilitates the primary productivity and subsequently leads to high depositional fluxes of organic matters and significant DO consumption in bottom water, which can exaggerate hypoxia. Relations between the nutrient loading and the hypoxic conditions have been well documented in many coastal hypoxic systems such as the Changjiang Estuary (Li et al., 2011; Ning et al., 2011), the Chesapeake Bay (Du and Shen, 2015; Hagy et al., 2004), and the northern Gulf of Mexico (Forrest et al., 2011; Justić et al., 2003). On a global scale, *Diaz and Rosenberg* [2008] also demonstrates a 10-years lag between the observed declining DO concentrations in coastal oceans and the increased nitrogen fertilizer utilization. As a result, nutrient reduction has been proposed to alleviate hypoxia in many hypoxic systems (e.g., the Chesapeake Bay (Scavia et al. (2006)) and the northern Gulf of Mexico (Justić et al. (2003))).

（Position of Figure 1）

The Pearl River Estuary (PRE) is located on the Pearl River Delta (Figure 1a) and has a drainage area of 452,000 km^2. Previous studies have reported some summer hypoxic events in the Pearl River Estuary and explored the underlying mechanisms (e.g., Yin et al., 2004). Yin et al. (2004) suggests that stratification and estuarine circulations are two primary processes controlling the hypoxia in the Pearl River Estuary. Rabouille et al. (2008) compares the hypoxic conditions among four hypoxic systems and demonstrates the significance of tidal mixing to break hypoxia in the Pearl River Estuary. Zhang and Li (2010) further suggests that the contributions of biogeochemical processes to hypoxia in the Pearl River Estuary are also important. By conducting the oxygen balance analysis, they show that sediment oxygen demand is the dominant sink for oxygen. A more recent study by Wang et al. (2017) further points out that the balance of oxygen in the Pearl River Estuary is mainly controlled by the source and sink processes occurring in local and adjacent waters, among which the re-aeration and sediment oxygen demand determine the spatial distributions and durations of hypoxia in the Pearl River Estuary.

As a distinct river-dominated estuary, the Pearl River Estuary receives 3.3×10^{11} m^3 yr^{-1} of freshwater (Ou et al., 2009; Zhang and Li, 2010) along with a large amount of nutrients and organic matters from the Pearl River network (Figure 1a), i. e. 5.6×10^5 t yr^{-1} of dissolved inorganic nitrogen (DIN) and 9.9×10^3 t yr^{-1} of dissolved inorganic phosphorus (DIP) (Hu and Li, 2009), and 2.5×10^6 t yr^{-1} of particulate organic carbon (POC). Both dissolved inorganic nitrogen and phosphorus loadings have increased by about 60% from 1970 to 2000 and is predicted to increase by two times in 2050 due to the fast-growing agriculture and urbanization (Strokal et al., 2015). Understanding the response of hypoxia and oxygen dynamics to the changes in nutrient loading in the Pearl River Estuary is hence valuable for hypoxia prediction and management.

In addition to the nutrient loading, organic matters are another important form of anthropogenic inputs that influence the hypoxia in the estuary. The organic matters can fuel the sediment oxygen demand when deposited and mineralized in the sediment layers, which has been found to dominate the DO depletions within the bottom waters of the Pearl River Estuary (Yin et al., 2004; Zhang and Li, 2010). In coastal systems the organic matters are often derived from the dead phytoplankton (Green et al., 2006), while in the Pearl River Estuary the organic matters mainly originate from the riverine inputs (Ye et al., 2017; Yu et al., 2010). The distinct characteristics of the organic matter source suggest the importance of studying the impact of riverine organic matters on hypoxia in the Pearl River Estuary.

In some cases, the hypoxia may also be induced by the advection of low-oxygen waters (Grantham et al., 2004; Montes et al., 2014; Wang, 2009; Wang et al., 2012). For example, Wang (2009) demonstrates that the hypoxia development in the Changjiang estuary is largely due to the Taiwan Warm Current bringing low–oxygen waters to the hypoxic zone. As to the Pearl River Estuary, the impact of riverine input of low-oxygen waters on hypoxia is also worth investigation considering the large amount of river discharge entering the estuary and that there has been hypoxia observed in its upper reaches(He et al., 2014).

Collectively the previous studies show that both natural and anthropogenic processes greatly contribute to hypoxia in the Pearl River Estuary. Understanding the respective roles of these two types of processes is important to faithfully predict future hypoxic events under the enhanced human activities and climate variations, which is useful for designing effective management strategies to prevent or remediate the hypoxic conditions in the Pearl River Estuary. Here we focus on the role of human activities, i.e. different anthropogenic inputs, on hypoxia and oxygen dynamics in the Pearl River Estuary, whereas the role of natural processes will be reported in our future works. Specifically, we explore the impacts of varying anthropogenic inputs (riverine nutrients, organic matter, and DO) on hypoxia and oxygen dynamics in the Pearl River Estuary by using a three-dimensional coupled physical-biogeochemical model. The physical modulation method introduced in Wang et al., (2017) is applied to isolate the effects of each oxygen source and sink processes and to elucidate their interactions in this shallow and river-dominated estuarine system.

2. Method

2.1 Model description and validation

2.1.1 Model description

Physical model

Our physical model is a 1D-3D coupled model developed and configured for the Pearl River-Estuary system (Figure 1b, c) (Hu and Li 2009; Hu et al. 2011). In order to incorporate the river network and the coastal areas in a single modeling system, the 1-D river network model is dynamically coupled with the 3-D estuarine model by exchanging the quantities through the eight outlets (i.e. Humen, Jiaomen, Hongqili, Hengmen, Modaomen, Jitimen, Hutiaomen, and Yamen; see Figure 1a for their locations).

The 1-D model solves the Saint Venant equations of mass and momentum conservation in the well-mixed river network. The model domain (Figure 1b) encompasses 299 major branches of the Pearl River network with 1726 computational cross-sections and 189 nodes. The five upper boundaries (i.e. Shizui, Gaoyao, Shijiao, Laoyagang, and Boluo; see Figure 1a for their locations) are specified by the real-time river discharge or water levels, while the eight lower boundaries (the eight outlets) use the water levels obtained from the 3-D model.

The 3-D model is based on the Estuaries and Coastal Ocean Model with Sediment Module (ECOMSED; HydroQual (2002)) that has been extensively used to study the hydrodynamics in estuaries. The model has 183x186 horizontal grid cells with a resolution ranging from 400 m inside the Lingdingyang Bay to 4 km near the open boundaries (Figure 1c), and has 16 terrain-following sigma layers with refined resolution near the surface and bottom layers. The horizontal mixing is parameterized by a Smagorinsky-type formula and the vertical mixing is calculated by the Mellor-Yamada level 2.5 turbulent closure model (Mellor and Yamada, 1982). The 3-D model is forced by the 6 hourly winds and 3 hourly surface heat fluxes from the ERA-interim (the Interim ECMWF Re-Analysis, http://www.ecmwf.int/en/research/climate-reanalysis/era-interim). Three open boundaries are specified by a monthly averaged profile of salinity and temperature (Hu and Li, 2009). Tides are introduced at the open boundaries using the water levels from the Oregon State University Tidal Data Inversion Software (OTIS). Freshwater inputs from the Pearl River network to the 3-D model use the river discharges simulated by the 1-D model.

The physical model is run from 1 November 2005 to 31 December 2006. More detailed descriptions and configurations can be found in Hu et al. (2011) and Wang et al. (2017).

Water quality model

The water quality model coupled to the physical model is the Row-Column AESOP model (RCA; HydroQual (2004)) that solves the mass balance equations for 26 state variables involved in five interactive cycles (i.e. the nitrogen cycle, the phosphorus cycle, the carbon cycle, the silicon cycle, and the oxygen dynamics). Interactions between these state variables with atmosphere and sediment are illustrated in Figure 2.

（Position of Figure 2）

The equation of DO (mg O_2 L^{-1}) is given by:

$$\frac{\partial DO}{\partial t} + u\frac{\partial DO}{\partial x} + v\frac{\partial DO}{\partial y} + w\frac{\partial DO}{\partial z} - \frac{\partial}{\partial x}\left(E_{\mathrm{x}}\frac{\partial DO}{\partial x}\right) - \frac{\partial}{\partial y}\left(E_{\mathrm{y}}\frac{\partial DO}{\partial y}\right) - \frac{\partial}{\partial z}\left(E_{\mathrm{z}}\frac{\partial DO}{\partial z}\right)$$

Biogeosciences Discuss., https://doi.org/10.5194/bg-2018-134
Manuscript under review for journal Biogeosciences
Discussion started: 25 April 2018

$$= WCP + REA + SOD \quad (1)$$

where x and y represent the horizontal coordinates and z the vertical coordinate; *u*, *v*, and *w* (m s^{-1}) represent velocity components in *x*, *y*, and *z* coordinates, respectively; and E_x, E_y, and E_z (m s^{-2}) are dispersion coefficients. Here the velocity components and dispersion coefficients are computed by the physical model. The term *WCP* represents the gross DO production rates in the water column (mg O_2 L^{-1} day^{-1}), hereafter the water column production, which is the sum of photosynthesis, respiration, nitrification, and oxidation (detailed equations are referred to HydroQual (2004)). The magnitudes of oxidation and nitrification are relatively small, hence the water column production rates are mainly determined by the photosynthesis and respiration. In the Pearl River Estuary, the photosynthesis production rate often exceeds the combination of respiration, oxidation, and nitrification rates that the water column is an overall source for DO concentrations (Wang et al., 2017).

The term *REA* represents the re-aeration (mg O_2 L^{-1} day^{-1}) at the air-sea interface, given as:

$$REA = k_{\mathrm{a}}\theta_{\mathrm{a}}^{T-20}(DO_{\mathrm{sat}} - DO) \quad (2)$$

where DO_{sat} represents the DO concentration at saturation (mg O_2 L^{-1} day^{-1}) which is dependent on salinity and temperature; k_{a} is the surface mass transfer coefficient (day^{-1}); and θ_{a} is a temperature coefficient. Values for these parameters are referred to HydroQual (2004) and Zhang and Li (2010).

The term *SOD* represents the sediment oxygen demand (mg O_2 L^{-1} day^{-1}) at the water-sediment interface and Δz represents thickness of the respective bottom grid cell.

$$SOD = \frac{s(DO_{\mathrm{sed}} - DO)}{\Delta z} \quad (3)$$

where s represents transfer coefficient between the sediment and overlying water; DO_{sed} represents DO concentrations in the sediment layers. In the RCA model, a sediment flux module is incorporated to simulate the depositional flux of particulate organic matter, the diagenesis processes in the sediment, and the transportation of dissolved matters from the sediment to the overlying water (Figure 2). Values of the sediment oxygen demand are negative, indicating that the sediment oxygen demand is a sink for DO.

(Position of Table 1)

The simulation period for our water quality model is the same as the physical model. Results during July and August 2006 are obtained for analysis of the summer hypoxia in the Pearl River Estuary. Details of the model configurations and the data used are referred to Zhang and Li (2010) and Wang et al. (2017).

2.1.2 Model validation

The coupled physical-biogeochemical model has been validated against available observations during the summer of 2006 in Wang et al. (2017). Here we briefly summarize the validation results as below.

The model-data comparison of water elevation indicates that our physical model is able to reproduce the tidal variations and the spring-neap tidal cycles in the Pearl River Estuary, with the normalized root-mean-square difference (RMSD) falling within 0.30 of the standard deviation of the observations and the correlation coefficient exceeding 95%. Model simulated salinity and temperature fields were also validated by comparing with 146 profiles of salinity and temperature collected by estuary-wide monitoring cruise, which shows that our physical model is robust to reproduce the broad-scale features and intra-seasonal patterns of the main hydrodynamic features in the Pearl River Estuary.

For validation of biogeochemical fields, the simulated DO concentrations were validated against 53 oxygen profiles collected at 4 different cruises and distributed estuary-wide. The point to point comparisons show that the simulated DO concentrations agree well with observations, with the normalized RMSD below 0.8 standard deviation of the observations and the vast majority (85%) of the normalized errors falling within 1 standard deviation of the observations. Model-data comparisons of bottom DO concentrations further show that the model is able to reproduce the spatial distribution of the observed bottom DO and hypoxia. We have also assessed model skills in resolving source and sink processes associated with DO concentration. We found that the simulated spatial distributions and magnitudes of the re-aeration, respiration, and the sediment oxygen demand rates are similar with those of previous observational studies (see Table 3 in Wang et al. 2017). The simulated chlorophyll-a, primary productivity and particulate organic carbon, which largely determine the respiration and the sediment oxygen demand rates (Zhang and Li, 2010), are also consistent with historical estimations. This suggests that our model is able to reproduce the oxygen dynamics properly.

In short, the model validation in Wang et al. (2017) indicate that our coupled physical-biogeochemical model is robust to simulate the hydrodynamics and biogeochemical cycles in the Pearl River Estuary and is skillful in simulating summer hypoxia in 2006.

2.2 The physical modulation method

The DO exhibits non-conservative behavior during the mixing in the estuary because of the oxygen source and sink processes described in Section 2.1.1 (Figure 3a). As shown in Figure 3b, the DO concentrations are controlled by both the conservative (represented by the theory mixing curve) and the non-conservative effects (represented by the shading areas). The conservative effects are associated with physical advection and diffusion, while the non-conservative effects are due to the oxygen source and sink processes (i.e. re-aeration, the water column production, and the sediment oxygen demand). Quantifying the relative contributions of the different effects is important to understand the DO dynamics during the mixing in the estuary. In a 0-D system, the non-conservative effects can be easily estimated as the products of time intervals and rates of corresponding source and sink processes. However, in a riverine dominated estuary such as the Pearl River Estuary, this estimation is not straightforward. This is because the DO concentrations can not only be affected by the source and sink processes occurring in local waters, but also by those in the adjacent waters (Wang et al. 2017). Moreover, these source and sink processes are nonlinearly interacted, which increases the complexity of the oxygen dynamics responding to different external forcing. To address these problems, the physical modulation method, introduced in Wang et al. (2017) to depict the modulation of effects of source and sink processes on DO distributions due to physical transport, is applied here to isolate the conservative and non-conservative effects on DO concentrations. In this study, the physical modulation method is incorporated into the water quality model dynamically by explicitly including four numerical oxygen species as model tracers to track the oxygen supply or removal by the lateral boundary conditions (DO_{BC}), air-sea re-aeration (DO_{REA}), water column production (DO_{WCP}), and sediment oxygen demand (DO_{SOD}), respectively (Figure 3a). Equations of the four numerical oxygen species are given as below:

$$\frac{\partial DO_{\mathrm{BC}}}{\partial t} + tran(DO_{\mathrm{BC}}) = 0 \qquad (4)$$

Biogeosciences Discuss., https://doi.org/10.5194/bg-2018-134
Manuscript under review for journal Biogeosciences
Discussion started: 25 April 2018

$$\frac{\partial DO_{\mathrm{REA}}}{\partial t} + tran(DO_{\mathrm{REA}}) = REA \quad (5)$$

$$\frac{\partial DO_{\mathrm{WCP}}}{\partial t} + tran(DO_{\mathrm{WCP}}) = WCP \quad (6)$$

$$\frac{\partial DO_{\mathrm{SOD}}}{\partial t} + tran(DO_{\mathrm{SOD}}) = SOD \quad (7)$$

and

$$DO = DO_{\mathrm{BC}} + DO_{\mathrm{REA}} + DO_{\mathrm{WCP}} + DO_{\mathrm{SOD}} \quad (8)$$

$$tran(DO) = tran(DO_{\mathrm{BC}}) + tran(DO_{\mathrm{REA}}) + tran(DO_{\mathrm{WCP}}) + tran(DO_{\mathrm{SOD}}) \quad (9)$$

where $tran$ represents the physical transport processes, i.e. the advection $(u\frac{\partial}{\partial x} + v\frac{\partial}{\partial y} + w\frac{\partial}{\partial z})$ and diffusion $(-\frac{\partial}{\partial x}\left(E_{\mathrm{x}}\frac{\partial}{\partial x}\right) - \frac{\partial}{\partial y}\left(E_{\mathrm{y}}\frac{\partial}{\partial y}\right) - \frac{\partial}{\partial z}\left(E_{\mathrm{z}}\frac{\partial}{\partial z}\right))$; REA, WCP, and SOD represent the re-aeration, water column production, and sediment oxygen demand obtained from the water quality model at each time step.

(Position of Figure 3)

According to Eq. 4, the DO_{BC} concentrations are only controlled by the advection and diffusion processes. By assigning the initial conditions and lateral boundary conditions of DO_{BC} the same as those for DO, the mixing curve of DO_{BC} will overlap the theory mixing curve shown in Figure 3b. It follows that the DO_{BC} represents the conservative effects, while the DO_{REA}, DO_{WCP}, and DO_{SOD} that include oxygen source or sink term represent the non-conservative effects.

The Eqs. 8 and 9 suggest that the DO concentration and its transport flux equal the sum of the concentrations and transport fluxes of the four DO species, respectively, the validity of which has been tested and confirmed in Wang et al. (2017). They show that there is little discrepancy between the DO concentrations calculated by Eq. (9) and Eq. (1), with 97% of the differences within the range of -2%~6% of the averaged DO concentrations. The hourly time series of domain-averaged DO calculated by the physical modulation method also agree well with that calculated by the water quality model with the R-square coefficient > 0.99 and the regression slope close to 1:1. In addition, the horizontal advective fluxes, vertical advective fluxes, and vertical diffusive fluxes calculated by the physical modulation method are found to agree well with the respective fluxes calculated by the water quality model, indicating that the physical modulation method is able to satisfactorily reproduce the physical transport processes of DO.

2.3 Model experiments

We conducted three groups of sensitivity experiments to study the response of hypoxia and oxygen dynamics to different scenarios of riverine inputs (Table 1). Each group has two simulations, where the concentration of one type of riverine inputs at river outlets is decreased and increased by 50%, respectively. In the Cont simulation, the DO concentration in Humen outlet, the largest river outlet in the Pearl River Estuary, is set to 4 mg L^{-1} based on observations nearby. The RivDO-50% simulation, where DO concentration is decreased by 50% to 2 mg L^{-1}, represents the scenario where hypoxia has developed in the river outlet as hypoxia has been previously reported in the upstream of Humen outlet (He et al., 2014). In contrast, the RivDO+50% simulation, where the DO concentration from the river network is increased by 50% to be close to that from the open boundaries, represents the scenario where the riverine input of DO is free from the anthropogenic impact. As to nutrient simulations, the RivNtr+50% simulation represents the scenario in 2050 with the predicted increase in nutrient input, whereas the RivNtr-50% simulation represents the scenario in 1970 when riverine nutrient input is lower and hypoxia has not been observed in the Pearl River Estuary (Zhang et al. 2013). Note that in the nutrient simulations, concentrations of all nutrients (including dissolved silica, dissolved inorganic phosphorus, ammonia nitrogen, and nitrite and nitrate nitrogen) are set to vary at the same percentage that the effects of different combinations of changes in nutrients are not considered here. The response of hypoxia and oxygen dynamics to varying riverine inputs in July and August 2006 are analyzed and discussed.

(**Position of Table 1**)

The hypoxic extent in different simulations is quantified by the expected hypoxic area and hypoxic volume:

$$Hypoxic\ area = \sum p * \Delta s \tag{10}$$

$$Hypoxic\ volume = \sum p * \Delta v \quad (11)$$

where Δs, Δv, and p are the area, the volume, and the hypoxic frequency of each model grid. The hypoxic frequency p is calculated by:

$$p = \frac{N_{\mathrm{h}}}{N_{\mathrm{s}}} * 100\% \quad (12)$$

where N_{h} is the number of hours when hypoxia occurs, and N_{s} is the total number of hours during July and August 2006. In this study, the threshold of hypoxia is defined as 3 mg L^{-1} (Luo et al., 2008; Rabalais et al., 2010).

Finally, by using the physical modulation method, we can quantify the relative contributions of different source and sink processes to the changes in DO by:

$$\Delta DO = \Delta DO_{\mathrm{BC}} + \Delta DO_{\mathrm{REA}} + \Delta DO_{\mathrm{WCP}} + \Delta DO_{\mathrm{SOD}} \quad (13)$$

3. Results

3.1 Response of hypoxia and oxygen dynamics to riverine DO inputs

Figure 4a, d show that in the 'Cont' simulation the shelf off the Modaomen sub-estuary is the high hypoxic frequency zone (HFZ) that has relatively lower DO concentrations and higher hypoxic frequency. Unlike the large spatial extent of hypoxia in the Changjiang Estuary (Wang, 2009; Wang et al., 2012) and the northern Gulf of Mexico (Rabouille et al., 2008), the hypoxia in the Pearl River Estuary is intermittent and confined to a small area (~217 km^2). In the 'RivDO-50%' simulation, the spatial distribution of DO concentrations is similar to that in the 'Cont' simulation except that hypoxia occurs near the river outlets associated with the low-oxygen waters discharged from the upstream river network (Figure 4b). As a result, the expected hypoxic extent remarkably increases at the region near the river outlets in 'RivDO-50%' (Figure 4e).

We have also examined the impact of reducing riverine DO on region further away from the river by excluding the hypoxic region near the river outlets when calculating hypoxic extent. In this case the expected hypoxic area in 'RivDO-50%' is 2% higher than that in the 'Cont' simulation (Figure 5a) while the hypoxic volume is 26% higher, indicating that the thickness of hypoxic water is increased in 'RivDO-50%'. In contrast, the 'RivDO+50%' simulation produces higher bottom DO concentrations in the high hypoxic frequency zone, leading to reductions of hypoxic area and volume by 23% and 30%, respectively (Figure 5a).

(Position of Figure 4)

(Position of Figure 5)

(Position of Figure 6)

To provide further insight into the response of different oxygen species to varying riverine DO inputs, the spatial distributions of DO_{BC} and DO_{REA} in the bottom water are shown in Figure 6. Differences in DO_{WCP} and DO_{SOD} concentrations between simulations are much smaller (Figure 5b) and hence omitted here. Halving the riverine DO inputs in the 'RivDO-50%' simulation yields lower DO_{BC} concentrations (Figure 6b) but higher DO_{REA} in the bottom water (Figure 5b and Figure 6d). As shown in Figure 5b, the decrease in DO_{BC} concentrations is largely balanced by the increase in DO_{REA} concentration in 'RivDO-50%' simulation, consequently reducing the magnitude of the changes in hypoxic extent responding to the reduced riverine DO input. In the contrary, the 'RivDO+50%' simulation leads to higher DO_{BC} concentrations (Figure 6c) but lower DO_{REA} in the bottom water (Figure 6f) that reduces the net increase in bottom DO (Figure 5b).

The re-aeration buffering effects can be explained by the surface apparent oxygen utilization (AOU, the difference between the actual DO concentration and its saturation at a known temperature and salinity). As shown in Eq. (2), the re-aeration is a function of surface AOU. Halving the riverine DO inputs decreases the DO concentrations in entire water column and therefore increases the surface AOU due to physical dilution, which ultimately results in an increase in re-aeration rate. In our model simulations, the surface domain-averaged saturated DO concentration is ~7.42 mg L^{-1}, while the surface domain-averaged DO concentration in 'Cont' and 'RivDO-50%' simulations are 6.81 and 6.57 mg L^{-1}, respectively. Surface AOU for the 'RivDO-50%'

simulation is 39% higher than that for the 'Cont' simulation, which is consistent with the 38% increase in re-aeration rate for the 'RivDO-50%' simulation.

3.2 Response of hypoxia and oxygen dynamics to riverine nutrient inputs

As shown in Figure 5a, perturbing riverine nutrient inputs by 50% has relatively weak impact on hypoxic extent (changes are within 10%). Among all the oxygen sink and source processes, the water column production and re-aeration are the two that are most sensitive to variations in nutrient inputs. Halving the nutrient inputs by 50% in the 'RivNtr-50%' simulation remarkably reduces the primary production and water column production rates, which in turn increases the surface AOU that facilitates the re-aeration. The increase in DO_{REA} to the bottom water via vertical diffusion offsets ~60% of the total DO loss associated with the reduced nutrient inputs in the high hypoxic frequency zone (Figure 5c). In contrast, the 'RivNtr+50%' simulation yields higher water column production and lower re-aeration rate, with the changes of the two balance each other, and hence only leads to 4% and 3% decreases in hypoxic area and hypoxic volume, respectively in relative to the 'Cont' simulation.

3.3 Response of hypoxia and oxygen dynamics to riverine POC inputs

As shown in Figure 5, perturbing the riverine inputs of particulate organic carbon by 50% leads to significant changes in DO concentrations and hypoxic extent. In the 'RivPOC-50%' simulation, the DO concentration increases by 0.56 mg L^{-1} in the high hypoxic frequency zone and the hypoxic area and hypoxic volume decrease by 50% and 64%, respectively. In the contrary, increasing the inputs of particulate organic carbon in 'RivPOC+50%' simulation leads to significant decrease in the DO concentration, causing an extension of hypoxic area by 64% and a doubling of hypoxic volume (Figure 5a).

As to oxygen dynamics, a 50% decrease in riverine inputs of particulate organic carbon results in significant decline in the sediment oxygen demand rate and increase in the water column production rate (Figure 5d) because the lowerinputs of particulate organic carbon weakens the light attenuation in PRE. The combination of lower sediment oxygen demand and higher water column production rates increases oxygen concentration by 0.81 mg L^{-1} in the bottom waters of the high hypoxic frequency zone. However, decreasing the riverine inputs of particulate organic carbon simultaneously weakens the re-aeration due to the decreased surface AOU. As a result, almost 27% of the increased DO concentrations is offset by the decreased re-aeration

Biogeosciences Discuss., https://doi.org/10.5194/bg-2018-134
Manuscript under review for journal Biogeosciences
Discussion started: 25 April 2018

in the high hypoxic frequency zone. In contrast, increasing the riverine inputs of particulate organic carbon by 50% increases the sediment oxygen demand rates but weakens the water column production rates, which consequently reduces bottom water oxygen. However, 26% of the oxygen loss is offset by the enhanced re-aeration.

To understand the impacts of changing the riverine inputs of particulate organic carbon on the water column production rates, we further examine how phytoplankton growth responds to varying riverine inputs of particulate organic carbon. The equation of phytoplankton growth G_P can be written as:

$$G_P = G_{Pmax} \cdot G(T) \cdot G(I) \cdot G(N) \quad (14)$$

where G_{Pmax} represents the maximum growth rate at the optimum conditions; $G(T)$, $G(I)$, and $G(N)$ represent the temperature limitation, light limitation, and the nutrients limitation, respectively. These limitation coefficients are represented by non-dimensional scales and range from 0 to 1, with 0 representing no growth and 1 no limitation. The three POC simulations have identical physical processes and hence same temperature limitations. Table 2 shows that changing the riverine inputs of particulate organic carbon leads to little differences in nutrient limitation but much larger variations in light limitation. This suggests that the riverine inputs of particulate organic carbon can significantly affect the growth of phytoplankton and the impact is mainly through light shading effects.

(Position of Table 3)

Considering the important role of re-aeration in POC simulations, we further quantify how re-aeration responds to the sediment oxygen demand by conducting a diagnostic analysis of DO_{SOD} during the July and August. Three vertical layers are defined: the upper layer (top 20% of depth), middle layer (middle 60% of depth), and bottom layer (20% depth above the sediment). Note that horizontal diffusion is omitted in the diagnostic analysis because its magnitude is much smaller than other terms. As shown in Figure 7, high levels of the sediment oxygen demand at the bottom layer (0.55 mg L^{-1} day^{-1}) cause declines not only in the bottom DO concentrations but also in the upward advective DO fluxes. While horizontal advection compensates the oxygen loss by bringing oxygen from adjacent waters, the sediment oxygen demand can still draw down surface DO

Biogeosciences Discuss., https://doi.org/10.5194/bg-2018-134
Manuscript under review for journal Biogeosciences
Discussion started: 25 April 2018

indirectly by a rate of 0.13 mg L^{-1} day^{-1}, which causes a decline of 2.22 mg L^{-1} in DO concentrations in the surface layer. Figure 8 shows the relative contributions of the sediment oxygen demand and the water column production rates to the changes of surface DO. The positive values of $\Delta(-DO_{SOD})$ and $\Delta(DO_{WCP})$ represent the increased DO concentrations caused by the changes of the sediment oxygen demand and the water column production, respectively. In the 'RivPOC-50%' simulation, decreasing the POC inputs decreases the sediment oxygen demand rate and increases the water column production rate, which increase the DO concentrations in the surface layer. As a result, the re-aeration is weakened, especially the west of lower estuary (Figure 8a).

(Position of Figure 7)

(Position of Figure 8)

4. Discussion

Previous model results have shown that the hypoxia in the Pearl River Estuary is confined to about 217 km^2 and intermittent due to the quick water exchange rates (Rabouille et al., 2008) and the destratification associate with tidal mixing (Zhang and Li, 2010). A more recent study by Wang et al. (2017) suggests that the re-aeration supply oxygen to surface water that enhances DO gradient between the surface and lower water layers, facilitating the surface DO_{REA} to penetrate to bottom water through vertical diffusion and compensate the oxygen loss by the sediment oxygen demand. Wang et al (2017) shows that nearly 28% of the surface DO_{REA} can reach the bottom layer to exert a strong constrain on the spatial extent and duration of hypoxia in the Pearl River Estuary. When turning off the re-aeration, the high sediment oxygen demand rate in the high hypoxic frequency zone as well as the west of the lower estuary lead to persistent hypoxia covering an area of over 3,000 km^2 in the Pearl River Estuary. In this study, we performed a suite of numerical experiments to quantify the relative contributions of different anthropogenic inputs to hypoxia and oxygen dynamics in the Pearl River Estuary.

4.1 Relative contributions of different anthropogenic inputs

Numerical experiments show that the hypoxia in the Pearl River Estuary is most sensitive to the riverine inputs of particulate organic carbon rather than the nutrient loading (Figure 5a). This is distinct from other hypoxic systems such as the Chesapeake Bay (Hagy et al., 2004) and the northern Gulf of Mexico (Justić et al., 2003) that observe close relation between nutrient loading and hypoxia. We attribute the difference to the different physical and biogeochemical processes regulating the hypoxic conditions in these systems (Table 4). In the Chesapeake Bay, the dominant oxygen sink leading to hypoxia is the water column respiration, which is associated with high primary production stimulated by the excessive nutrient loading (Hong and Shen, 2013). In contrast, the bottom water DO depletions are dominated by the sediment oxygen demand in the northern Gulf of Mexico (Murrell and Lehrter, 2011; Yu et al., 2015) and the Pearl River Estuary (Yin et al., 2004; Zhang and Li, 2010), although the relative contributions of marine POC (i.e. the particulate organic carbon generated by settling of phytoplankton after death) versus terrestrial POC to the sediment oxygen demand are different in the two systems. In the northern Gulf of Mexico, the marine source serves as the major source of particulate organic carbon (Green et al., 2006), which means increasing the nutrient loading can facilitate the sediment oxygen demand rates by increasing the depositional fluxes of dead phytoplankton that consequently promote the formation of hypoxia. However, in the Pearl River Estuary, the sediment oxygen demand is primarily fueled by the terrestrial POC (Ye et al., 2017; Yu et al., 2010) which is set unchanged in all our nutrient simulations. Compared with the Mississippi River (~95 d; Table 3), the residence time in the Pearl River Estuary is much shorter (3-5 d), implying weaker degradation and deposition of the terrestrial POC. Moreover, the Pearl River Estuary has relatively low primary productivity due to the phosphorus limitation (DIN:DIP=126; Table 4) and shading effects of suspended sediments.

(Position of Table 4)

The relative contributions of terrestrial versus marine POC inputs have long been a topic of debate in the Pearl River Estuary. Some studies suggest that terrestrial source dominate in wet seasons due to the high river discharges (Ye et al., 2017; Yu et al., 2010), while others argue that marine inputs can also play an important role (Guo et al., 2015; Su et al., 2017). Previous studies (Guo et al., 2015; Hu et al., 2006; Ye et al., 2017) show that the ratios of terrestrial inputs to marine inputs have distinct spatial and seasonal variabilities in the Pearl River Estuary. Generally, the terrestrial contributions dominate inside the estuary and gradually decrease seaward as the impact of the river discharges weakens (Hu et al., 2006; Jia and Peng, 2003). In our study, the high hypoxic frequency zone is near the Modaomen sub-estuary which receives high depositional fluxes of riverine particulate organic carbon. Therefore, the land-derived particulate organic carbon has dominant contributions to the summer hypoxia in the high hypoxic frequency zone.

4.2 The importance of re-aeration in PRE

Model results also highlight the importance of re-aeration in regulating DO dynamics and hypoxia migration in the Pearl River Estuary. On the one hand, the re-aeration together with the sediment oxygen demand is the most important process controlling DO dynamics. On the other hand, the re-aeration responds rapidly to the perturbations of riverine inputs, which moderates the DO changes impacted by the perturbations. A conceptual diagram of these processes is illustrated in Figure 9. Compared with other hypoxic systems, in the Pearl River Estuary, the re-aeration is of great significance because of the shallow topography and the strong re-aeration that enables the surface re-aeration penetrating to the bottom water. Re-aeration thus can greatly influence the formation and spatial migration of hypoxia under the perturbations of riverine inputs. The strong re-aeration in the Pearl River Estuary is also a result of the shallow topography which allows the bottom sediment oxygen demand to indirectly affect the surface DO by decreasing the upward DO advective fluxes. As we have described in section 3.3, the bottom sediment oxygen demand can lead to a decrease in surface DO concentrations by 2.22 mg L^{-1}. If turned off the sediment oxygen demand, the surface AOU would change from 0.61 from -1.61 mg L^{-1}, and re-aeration change from 0.55 mg L^{-1} day^{-1} to -1.45 mg L^{-1} day^{-1}. This indicates that the sediment oxygen demand shifts the re-aeration from a strong oxygen sink to a strong source. One counter-example is the northern Gulf of Mexico, where the hypoxic zone is deeper such that the surface water and bottom hypoxic water is dettached. Also, the observed sediment oxygen demand varies from 0.06 to 0.70 g m^{-2} day^{-1} in the summer season in the northern Gulf of Mexico (Murrell and Lehrter (2011)), which is much lower than those in the Pearl River Estuary (0.72~3.89 g m^{-2} day^{-1}; Chung et al. (2004)). These characteristics and the high primary productivity in the northern Gulf of Mexico lead to the supersaturated DO concentrations in the surface water and that the re-aeration is primarily an outgassing process (Yu et al., 2015).

Biogeosciences Discuss., https://doi.org/10.5194/bg-2018-134
Manuscript under review for journal Biogeosciences
Discussion started: 25 April 2018

（**Position of Figure 9**）

5. Conclusion

This study uses a coupled physical-biogeochemical coupled model to simulate the DO dynamics and hypoxia in the Pearl River Estuary and investigate their responses to perturbations in riverine inputs. Results show that the hypoxia in the Pearl River Estuary has small spatial extent and strong intermittency in time due to the counterbalance of re-aeration and the sediment oxygen demand, and that perturbing riverine inputs has strong impact on DO dynamics and hypoxia. The hypoxic extent in the Pearl River Estuary is most sensitive to riverine input of particulate organic carbon, followed by oxygen and nutrients. This is different from other hypoxic systems because of the distinct physical and biogeochemical features in the Pearl River Estuary, i.e. the shallow topography, high water exchange rates and dominance of the sediment oxygen demand for DO depletions within bottom waters.

Model results also highlight the importance of re-aeration and its buffering effects for the oxygen dynamics in the Pearl River Estuary. River-induced changes in source and sink processes can trigger an opposite shift in re-aerations by altering the surface AOU. In turn, the re-aeration can moderate the DO changes and hypoxia shifts responding to the changes in the oxygen source and sink processes. The important role of re-aeration in the Pearl River Estuary is due to the shallow waters in the estuary. Firstly, the shallow waters enable the re-aeration to penetrate to bottom waters to compensate the DO loss by the sediment oxygen demand. Secondly, due to the shallow waters, the sediment oxygen demand can affect the surface DO indirectly by decreasing the surface AOU and consequently shifting re-aeration from an oxygen sink to a strong oxygen source.

Acknowledge

This work was supported by the National Natural Science Foundation of China (grant no: 41306105), the Guangdong Natural Science Foundation (grant no: 2014A030313169), the Science and Technology Planning Project of Guangdong Province, China (grant no: 2014A020217003), and the Fundamental Research Funds for the Central Universities (grant no: 17lgzd20).

Biogeosciences Discuss., https://doi.org/10.5194/bg-2018-134
Manuscript under review for journal Biogeosciences
Discussion started: 25 April 2018

Reference

Chung, J., Gary, C. and Heinke, W.: Pearl River Estuary Pollution Project (PREPP), Cont. Shelf Res., 24(16), 1739–1744, 2004.

Diaz, R. J. and Rosenberg, R.: Spreading Dead Zones and Consequences for Marine Ecosystems, Science (80-.)., 321(5891), 926–929, doi:10.1126/science.1156401, 2008.

Du, J. and Shen, J.: Decoupling the influence of biological and physical processes on the dissolved oxygen in the Chesapeake Bay, J. Geophys. Res. Ocean., 120(1), 78–93, doi:10.1002/2014JC010422, 2015.

Forrest, D. R., Hetland, R. D. and Dimarco, S. F.: Multivariable statistical regression models of the areal extent of hypoxia over the Texas-Louisiana continental shelf, Environ. Res. Lett., 6(4), doi:10.1088/1748-9326/6/4/045002, 2011.

Grantham, B. A., Chan, F., Nielsen, K. J., Fox, D. S., Barth, J. A., Huyer, A., Lubchenco, J. and Menge, B. A.: Upwelling-driven nearshore hypoxia signals ecosystem and oceanographic changes in the northeast Pacific, Nature, 429(6993), 749–754, doi:10.1038/nature02605, 2004.

Green, R. E., Bianchi, T. S., Dagg, M. J., Walker, N. D. and Breed, G. A.: An organic carbon budget for the Mississippi River turbidity plume and plume contributions to air-sea CO2 fluxes and bottom water hypoxia, Estuaries and Coasts, 29(4), 579–597, doi:10.1007/BF02784284, 2006.

Guo, W., Ye, F., Xu, S. and Jia, G.: Seasonal variation in sources and processing of particulate organic carbon in the Pearl River estuary, South China, Estuar. Coast. Shelf Sci., 167, 540–548, doi:10.1016/j.ecss.2015.11.004, 2015.

Hagy, J. D., Boynton, W. R., Keefe, C. W. and Wood, K. V.: Hypoxia in Chesapeake Bay, 1950–2001: Long-term change in relation to nutrient loading and river flow, Estuaries, 27(4), 634–658, doi:10.1007/BF02907650, 2004.

He, B., Dai, M., Zhai, W., Guo, X. and Wang, L.: Hypoxia in the upper reaches of the Pearl River Estuary and its maintenance mechanisms: A synthesis based on multiple year observations during 2000-2008, Mar. Chem., doi:10.1016/j.marchem.2014.07.003, 2014.

Hong, B. and Shen, J.: Linking dynamics of transport timescale and variations of hypoxia in the Chesapeake Bay, J. Geophys. Res. Ocean., 118(11), 6017–6029, doi:10.1002/2013JC008859, 2013.

Hu, J. and Li, S.: Modeling the mass fluxes and transformations of nutrients in the Pearl River Delta, China, J. Mar. Syst., 78(1), 146–167, doi:10.1016/j.jmarsys.2009.05.001, 2009.

Hu, J., Peng, P., Jia, G., Mai, B. and Zhang, G.: Distribution and sources of organic carbon, nitrogen and their isotopes in sediments of the subtropical Pearl River estuary and adjacent shelf, Southern China, Mar. Chem., 98(2–4), 274–285, doi:10.1016/j.marchem.2005.03.008, 2006.

Hu, J., Li, S. and Geng, B.: Modeling the mass flux budgets of water and suspended sediments for the river network and estuary in the Pearl River Delta, China, J. Mar. Syst., 88(2), 252–266, doi:10.1016/j.jmarsys.2011.05.002, 2011.

HydroQual, Inc.: A Primer for ECOMSED Version 1.3., HydroQual, Inc., Mahwah, NJ., 2002.

HydroQual, Inc.: User's Guide for RCA (Release 3.0)., HydroQual, Inc., Mahwah, NJ., 2004.

Jia, G.-D. and Peng, P.-A.: Temporal and spatial variations in signatures of sedimented organic matter in Lingding Bay (Pearl estuary), southern China, Mar. Chem., 82(1–2), 47–54, doi:10.1016/S0304-4203(03)00050-1, 2003.

Justić, D., Rabalais, N. N. and Turner, R. E.: Simulated responses of the Gulf of Mexico hypoxia to variations in climate and anthropogenic nutrient loading, J. Mar. Syst., 42(3–4), 115–126, doi:10.1016/S0924-7963(03)00070-8, 2003.

Li, X., Bianchi, T. S., Yang, Z., Osterman, L. E., Allison, M. A., DiMarco, S. F. and Yang, G.: Historical trends of hypoxia in Changjiang River estuary: Applications of chemical biomarkers and microfossils, J. Mar. Syst., 86(3–4), 57–68, doi:10.1016/j.jmarsys.2011.02.003, 2011.

Luo, L., Li, S. Y. and Wang, D. X.: Modelling of hypoxia in the Pearl River estuary in summer, Adv. Water Sci., 2008.

Mellor, G. L. and Yamada, T.: Development of a turbulence closure model for geophysical fluid problems, Rev. Geophys., 20(4), 851–875, doi:10.1029/RG020i004p00851, 1982.

Montes, I., Dewitte, B., Gutknecht, E., Paulmier, A., Dadou, I., Oschlies, A. and Garçon, V.: High-resolution modeling of the Eastern Tropical Pacific oxygen minimum zone: Sensitivity to the tropical oceanic circulation, J. Geophys. Res. Ocean., 119(8), 5515–5532, doi:10.1002/2014JC009858, 2014.

Murrell, M. C. and Lehrter, J. C.: Sediment and Lower Water Column Oxygen Consumption in the Seasonally Hypoxic Region of the Louisiana Continental Shelf, Estuaries and Coasts, doi:10.1007/s12237-010-9351-9, 2011.

Ning, X., Lin, C., Su, J., Liu, C., Hao, Q. and Le, F.: Long-term changes of dissolved oxygen, hypoxia, and the responses of the ecosystems in the East China Sea from 1975 to 1995, J. Oceanogr., doi:10.1007/s10872-011-0006-7, 2011.

Ou, S., Zhang, H. and Wang, D. X.: Dynamics of the buoyant plume off the Pearl River Estuary in summer, Environ. Fluid Mech., doi:10.1007/s10652-009-9146-3, 2009.

Quigg, A., Sylvan, J. B., Gustafson, A. B., Fisher, T. R., Oliver, R. L., Tozzi, S. and Ammerman, J. W.: Going West: Nutrient Limitation of Primary Production in the Northern Gulf of Mexico and the Importance of the Atchafalaya River, Aquat. Geochemistry, doi:10.1007/s10498-011-9134-3, 2011.

Rabalais, N. N., Díaz, R. J., Levin, L. A., Turner, R. E., Gilbert, D. and Zhang, J.: Dynamics and distribution of

Biogeosciences Discuss., https://doi.org/10.5194/bg-2018-134
Manuscript under review for journal Biogeosciences
Discussion started: 25 April 2018

natural and human-caused hypoxia, Biogeosciences, doi:10.5194/bg-7-585-2010, 2010.

Rabouille, C., Conley, D. J., Dai, M. H., Cai, W. J., Chen, C. T. A., Lansard, B., Green, R., Yin, K., Harrison, P. J., Dagg, M. and McKee, B.: Comparison of hypoxia among four river-dominated ocean margins: The Changjiang (Yangtze), Mississippi, Pearl, and Rhône rivers, Cont. Shelf Res., 28(12), 1527–1537, doi:10.1016/j.csr.2008.01.020, 2008.

Scavia, D., Kelly, E. L. a and Hagy, J. D.: A simple model for forecasting the effects of nitrogen loads on Chesapeake Bay hypoxia, Estuaries and Coasts, 29(4), 674–684, doi:10.1007/BF02784292, 2006.

Strokal, M., Kroeze, C., Li, L., Luan, S., Wang, H., Yang, S. and Zhang, Y.: Increasing dissolved nitrogen and phosphorus export by the Pearl River (Zhujiang): a modeling approach at the sub-basin scale to assess effective nutrient management, Biogeochemistry, doi:10.1007/s10533-015-0124-1, 2015.

Su, J., Dai, M., He, B., Wang, L., Gan, J., Guo, X., Zhao, H. and Yu, F.: Tracing the origin of the oxygen-consuming organic matter in the hypoxic zone in a large eutrophic estuary: The lower reach of the Pearl River Estuary, China, Biogeosciences, 14(18), 4085–4099, doi:10.5194/bg-14-4085-2017, 2017.

Wang, B.: Hydromorphological mechanisms leading to hypoxia off the Changjiang estuary, Mar. Environ. Res., 67(1), 53–58, doi:10.1016/j.marenvres.2008.11.001, 2009.

Wang, B., Wei, Q., Chen, J. and Xie, L.: Annual cycle of hypoxia off the Changjiang (Yangtze River) Estuary, Mar. Environ. Res., 77, 1–5, doi:10.1016/j.marenvres.2011.12.007, 2012.

Wang, B., Hu, J., Li, S. and Liu, D.: A numerical analysis of biogeochemical controls with physical modulation on hypoxia during summer in the Pearl River estuary, Biogeosciences, 14(12), 2979–2999, doi:10.5194/bg-14-2979-2017, 2017.

Ye, F., Guo, W., Shi, Z., Jia, G. and Wei, G.: Seasonal dynamics of particulate organic matter and its response to flooding in the Pearl River Estuary, China, revealed by stable isotope (δ 13 C and δ 15 N) analyses, J. Geophys. Res. Ocean., 1–22, doi:10.1002/2017JC012931, 2017.

Ye, H., Chen, C., Sun, Z., Tang, S., Song, X., Yang, C., Tian, L. and Liu, F.: Estimation of the Primary Productivity in Pearl River Estuary Using MODIS Data, Estuaries and Coasts, doi:10.1007/s12237-014-9830-5, 2014.

Yin, K., Lin, Z. and Ke, Z.: Temporal and spatial distribution of dissolved oxygen in the Pearl River Estuary and adjacent coastal waters, Cont. Shelf Res., 24(16), 1935–1948, doi:10.1016/j.csr.2004.06.017, 2004.

Yu, F., Zong, Y., Lloyd, J. M., Huang, G., Leng, M. J., Kendrick, C., Lamb, A. L. and Yim, W. W. S.: Bulk organic δ13C and C/N as indicators for sediment sources in the Pearl River delta and estuary, southern China, Estuar. Coast. Shelf Sci., 87(4), 618–630, doi:10.1016/j.ecss.2010.02.018, 2010.

Yu, L., Fennel, K., Laurent, A., Murrell, M. C. and Lehrter, J. C.: Numerical analysis of the primary processes controlling oxygen dynamics on the Louisiana shelf, Biogeosciences, doi:10.5194/bg-12-2063-2015, 2015.

Zhang, H. and Li, S.: Effects of physical and biochemical processes on the dissolved oxygen budget for the Pearl River Estuary during summer, J. Mar. Syst., 79(1–2), 65–88, doi:10.1016/j.jmarsys.2009.07.002, 2010.
Zhang, L. K., Qin, X. Q., Yang, H., Huang, Q. B. and Liu, P. Y.: Transported fluxes of the riverine carbon and seasonal variation in Pearl River basin, Huan jing ke xue, 34(34), 3025–3034, 2013.

Table list

Table 1. Overview of model experiments

Experiments	Description
Cont	Forced by the riverine inputs of monthly observed DO, nutrients and particulate organic carbon concentration from 2006 collected by the State Oceanic Administration
DO simulations	
RivDO-50%	Same as Cont simulation except the riverine DO inputs are decreased by 50%
RivDO+50%	Same as Cont simulation except the riverine DO inputs are increased by 50%
Nutrients simulations	
RivNtr-50%	Same as Cont simulation except the riverine nutrients inputs are decreased by 50%
RivNtr+50%	Same as Cont simulation except the riverine nutrients inputs are increased by 50%
POC simulations	
RivPOC-50%	Same as Cont simulation except the riverine inputs of particulate organic carbon are decreased by 50%
RivPOC+50%	Same as Cont simulation except the riverine inputs of particulate organic carbon are increased by 50%

Biogeosciences Discuss., https://doi.org/10.5194/bg-2018-134
Manuscript under review for journal Biogeosciences
Discussion started: 25 April 2018

Table 2. Comparisons of nutrient limitation and light limitation on the growth of phytoplankton for 'Cont' and two POC simulations. Values are averaged over the bottom layer of the Pearl River Estuary. The lower values represent the stronger limitation.

	Cont	**RivPOC-50%**	**RivPOC+50%**
Nutrient limitation	0.81±0.09	0.80±0.09	0.82±0.09
Light limitation	0.21±0.15	0.25±0.16	0.18±0.14

Table 3. Residence time, primary productivity, nutrients input, and nutrients ratios in the Pearl River Estuary and the northern Gulf of Mexico

	Period	Pearl River Estuary	Northern Gulf of Mexico
Residence Time (d)	Summer	3-5 [a]	~95 [a]
Primary productivity (mg m^{-2} day^{-1})	Summer	183.9–1,213 [b]	330-7,010 [c]
DIN loading (t d^{-1})	Annual	1531 [d]	1955 [d]
DIP loading (t d^{-1})	Annual	27 [d]	133 [d]
DIN:DIP (mol:mol)	Annual	126 [d]	33 [d]

[a] Rabouille et al. (2008)
[b] Ye et al. (2014)
[c] Quigg et al. (2011)
[d] Hu and Li (2009)

Biogeosciences Discuss., https://doi.org/10.5194/bg-2018-134
Manuscript under review for journal Biogeosciences
Discussion started: 25 April 2018

Figure caption

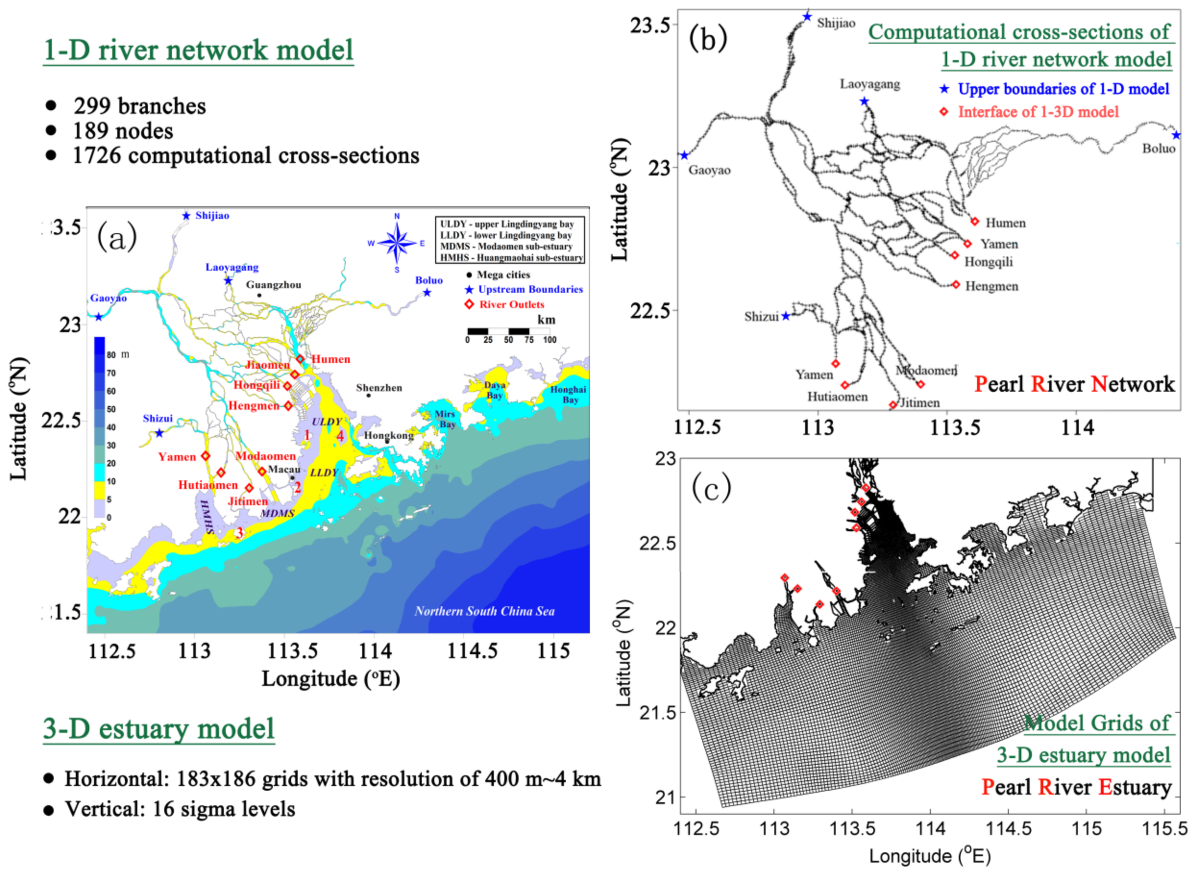

Figure 1 Maps showing (a) the Pearl River Delta with the Pearl River network and the Pearl River Estuary, (b) computational cross-sections for 1-D river network model, and (c) the model grid for 3-D estuary model. Italic numbers in Figure 1a represent islands which are not marked on the map: 1-Qiao island; 2-Hengqin island; 3-Gaolan island; and 4-Inner Lingding island.

Biogeosciences Discuss., https://doi.org/10.5194/bg-2018-134
Manuscript under review for journal Biogeosciences
Discussion started: 25 April 2018

Biogeosciences
Discussions
Open Access

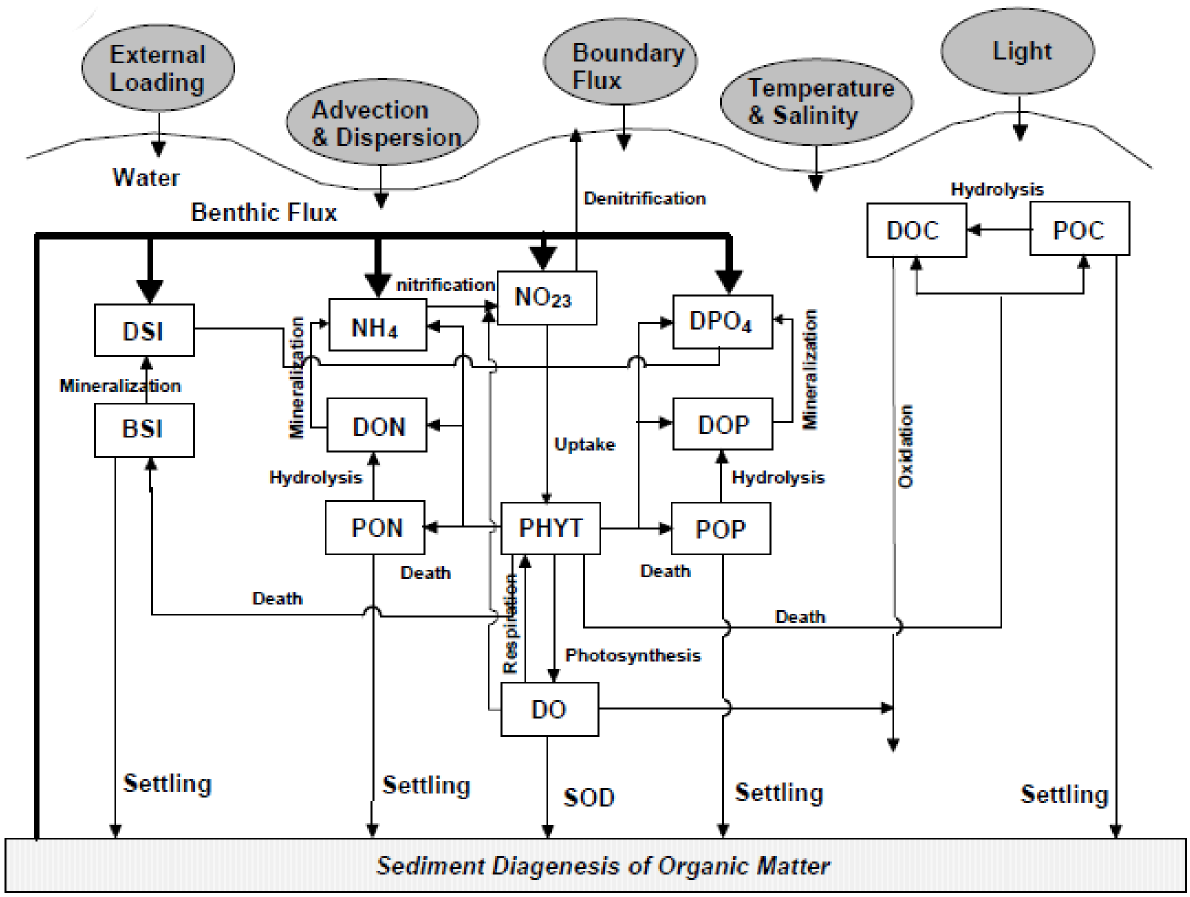

Figure 2 Conceptual framework for RCA model with a sediment flux module (Zhang and Li, 2010). DO represents dissolved oxygen; PHYT represents phytoplankton; POC represents particulate organic carbon; DOC represents dissolved organic carbon; NH_4 represents ammonia nitrogen; NO_{23} represents nitrite and nitrate nitrogen; PON represents particulate organic nitrogen; DON represents dissolved organic nitrogen; DPO_4 represents dissolved inorganic phosphorus; POP represents particulate organic phosphorus; DOP represents dissolved organic phosphorus; DSi represents dissolved silica; BSi represent biogenic silica; and SOD represents sediment oxygen demand.

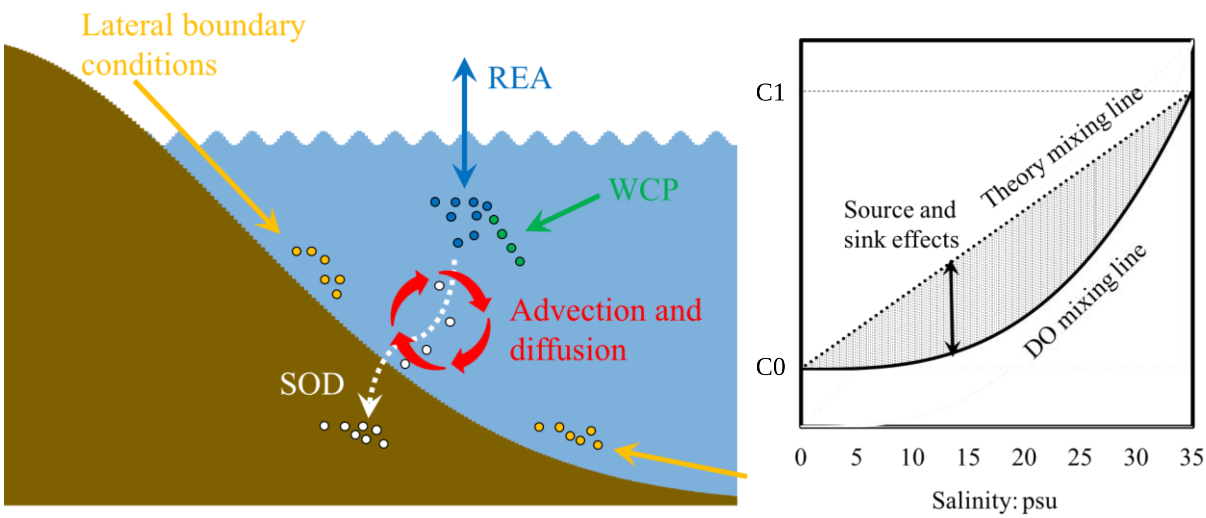

Figure 3 The schematic diagram illustrating the mixing process of dissolved oxygen in the estuary (a). The schematic plot for dissolved oxygen versus salinity (the solid black curve line) during the mixing in the estuary. C1 represents the concentrations in sea water, while C0 represents the concentrations in river water.

Biogeosciences Discuss., https://doi.org/10.5194/bg-2018-134
Manuscript under review for journal Biogeosciences
Discussion started: 25 April 2018

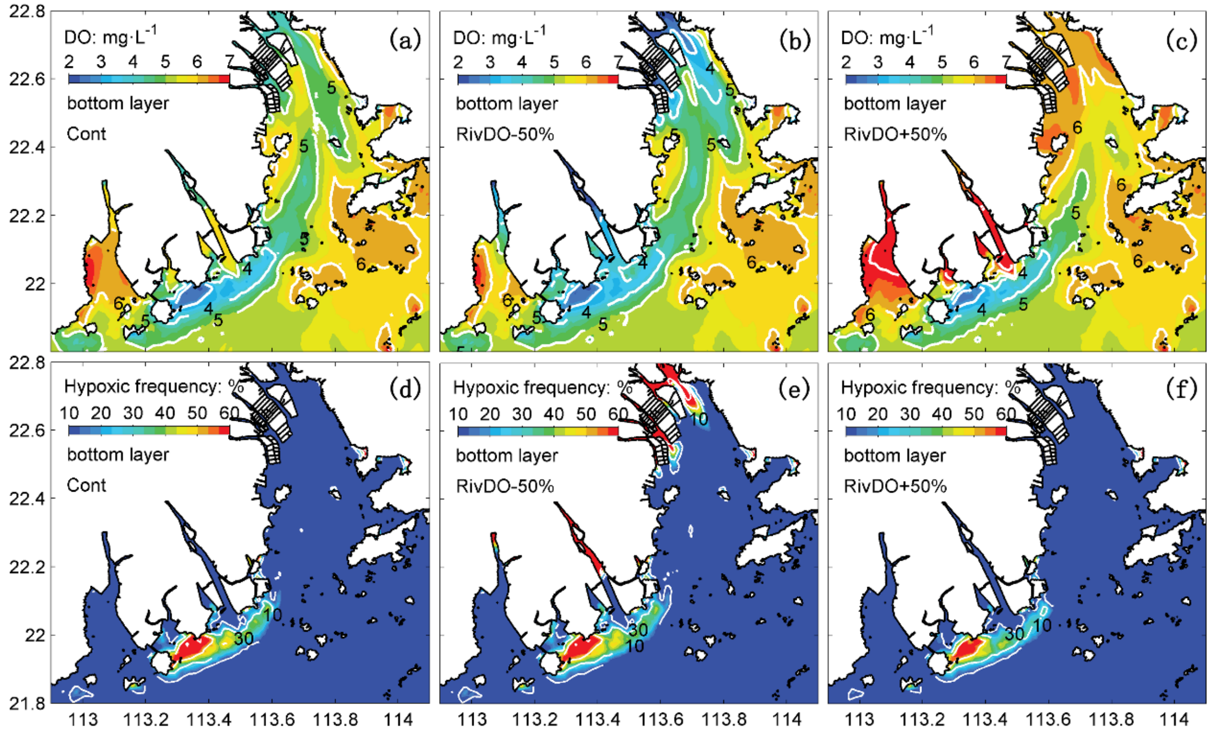

Figure 4 The spatial distribution of DO concentration and hypoxic frequency in the bottom layer for DO concentration simulations. The DO concentration is averaged over July and August 2006. The hypoxia is defined as DO concentraion below 3 mg L^{-1}.

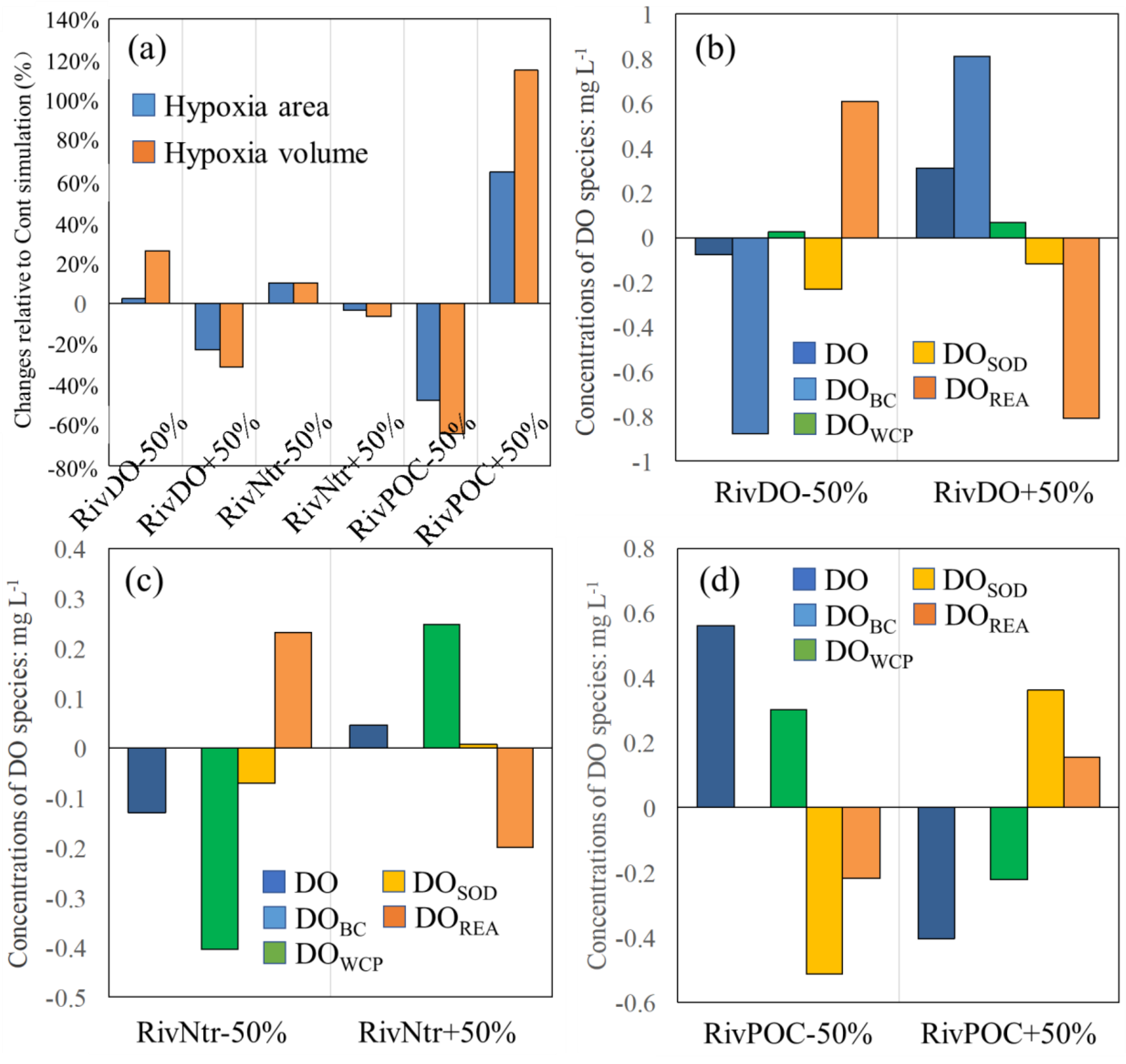

Figure 5 The percentage changes of the hypoxic area and hypoxic volume in each simulation in relative to the Cont simulation (a). The changes of each DO species averaged over the High hypoxic frequency zone in DO simulations (b), nutrient simulations (c), and POC simulations (d) in relative to the Cont simulation.

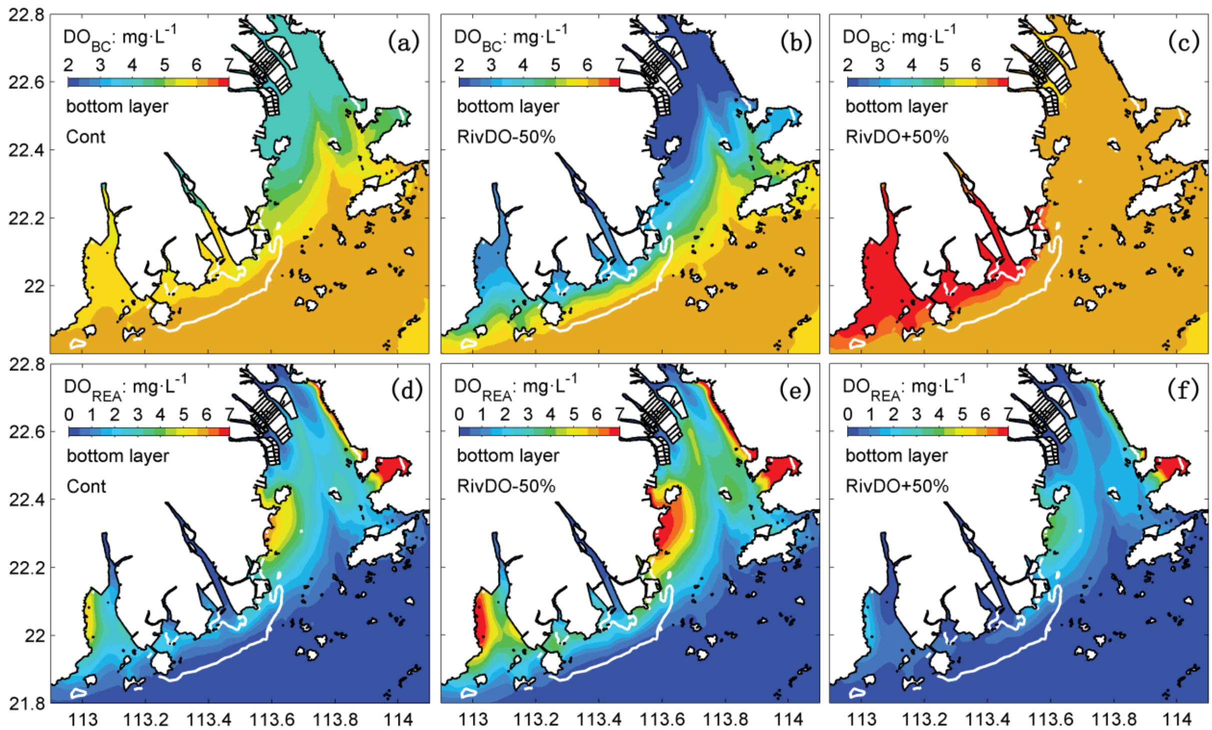

Figure 6 The spatial distribution of DO_{BC} and DO_{REA} concentrations at the bottom layer for three DO simulations.

Biogeosciences Discuss., https://doi.org/10.5194/bg-2018-134
Manuscript under review for journal Biogeosciences
Discussion started: 25 April 2018

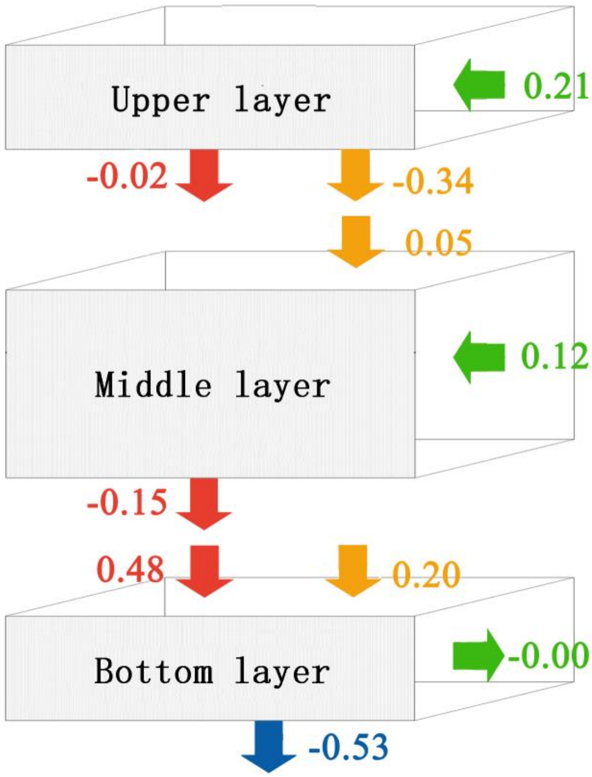

Figure 7 Budget of $-DO_{SOD}$ for the upper layer, middle layer, and bottom layer in the Pearl River Estuary for the 'Cont' simulation. Blue arrow represents sediment oxygen demand, red arrows represent the vertical diffusion, orange arrows represent vertical advection, and green arrows represent horizontal advection. Positive values mean the source effects while the negative values mean the sink effects of the sediment oxygen demand on DO concentrations. (unit: mg L^{-1} day^{-1})

Biogeosciences Discuss., https://doi.org/10.5194/bg-2018-134
Manuscript under review for journal Biogeosciences
Discussion started: 25 April 2018

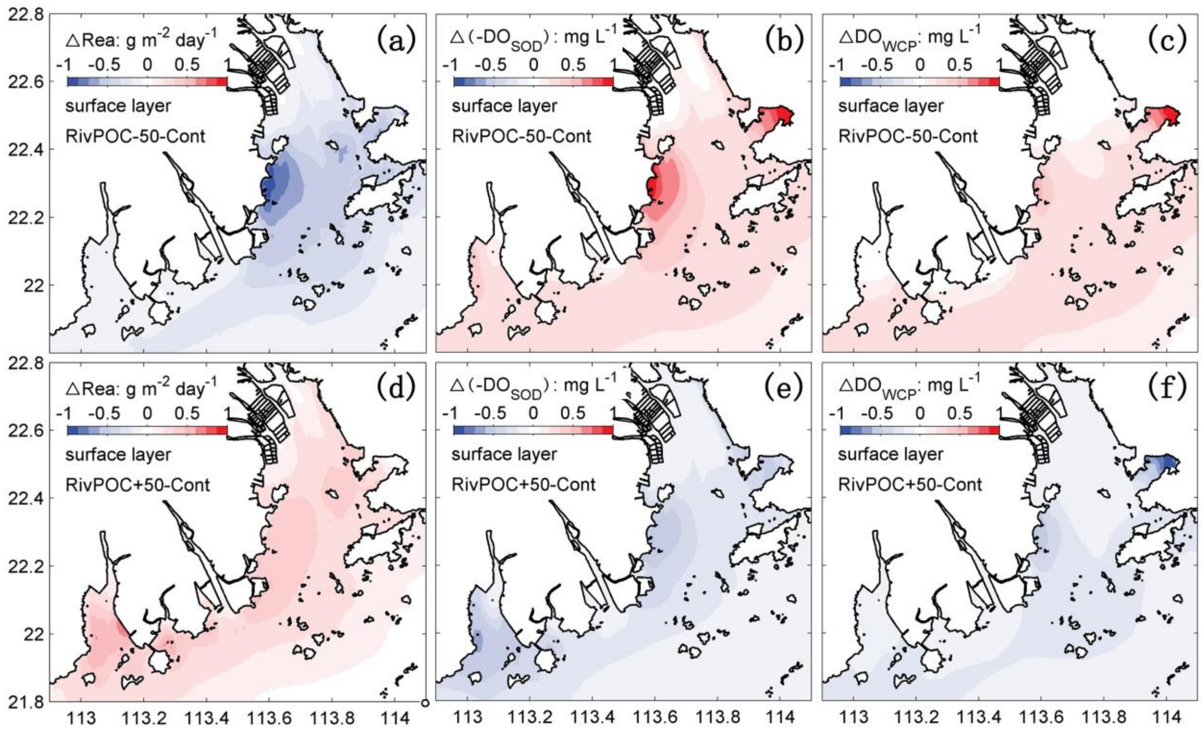

Figure 8 The changes in air-sea re-aeration rates, -DO_{SOD}, and DO_{WCP} concentrations in the surface layer with respect to the 'Cont' simulation (model-Cont). Positive values of ΔRea, $\Delta(-DO_{SOD})$ and ΔDO_{WCP} concentrations represent higher re-aeration rates, higher DO concentrations caused by the changes of the sediment oxygen demand rate and the water column production rate, respectively.

Biogeosciences Discuss., https://doi.org/10.5194/bg-2018-134
Manuscript under review for journal Biogeosciences
Discussion started: 25 April 2018

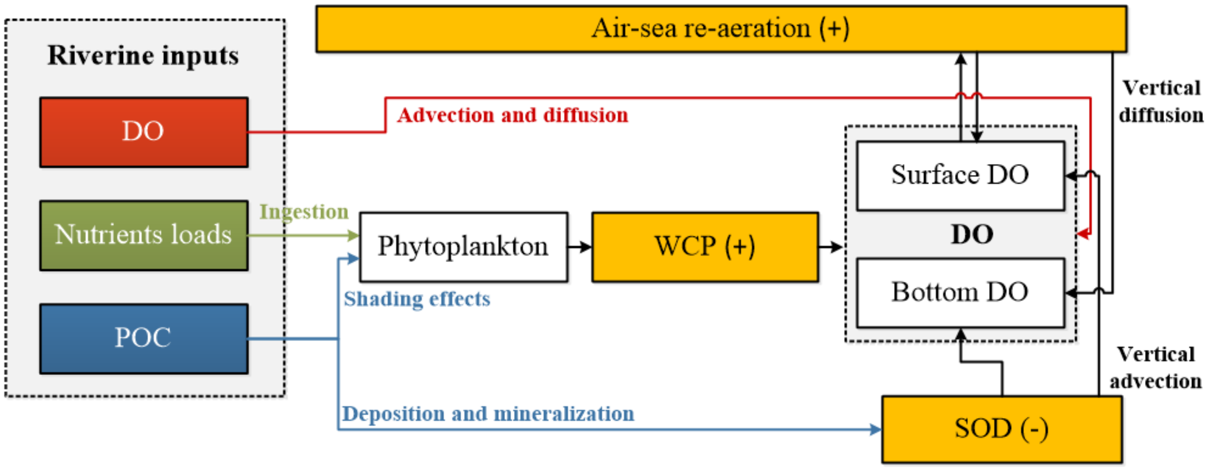

Figure 9 Conceptual schematic of the oxygen dynamics in response to riverine inputs in the Pearl River Estuary. The white boxes represent the state variables in the water body, the orange boxes represent the source and sink processes associated with the oxygen dynamics. The positive signs represent the sources while the negative signs represent the sinks for DO concentrations.